

Accepted Manuscript

Simulated Optimisation of Disordered Structures with Negative Poisson's Ratios

E.J. Horrigan, C.W. Smith, F.L. Scarpa, N Gaspar, A.A. Javadi, M.A. Berger, K.E. Evans

PII: S0167-6636(09)00087-8
DOI: [10.1016/j.mechmat.2009.04.008](https://doi.org/10.1016/j.mechmat.2009.04.008)
Reference: MECMAT 1707

To appear in: *Mechanics of Materials*

Received Date: 14 April 2008
Revised Date: 13 February 2009
Accepted Date: 15 April 2009

Please cite this article as: Horrigan, E.J., Smith, C.W., Scarpa, F.L., Gaspar, N., Javadi, A.A., Berger, M.A., Evans, K.E., Simulated Optimisation of Disordered Structures with Negative Poisson's Ratios, *Mechanics of Materials* (2009), doi: [10.1016/j.mechmat.2009.04.008](https://doi.org/10.1016/j.mechmat.2009.04.008)

This is a PDF file of an unedited manuscript that has been accepted for publication. As a service to our customers we are providing this early version of the manuscript. The manuscript will undergo copyediting, typesetting, and review of the resulting proof before it is published in its final form. Please note that during the production process errors may be discovered which could affect the content, and all legal disclaimers that apply to the journal pertain.



Simulated Optimisation of Disordered Structures with Negative Poisson's Ratios

Horrigan EJ, Smith CW[†], Scarpa FL*, Gaspar N, Javadi AA, Berger MA, Evans KE
School of Engineering, Computing and Mathematics, Harrison Building, University
of Exeter, North Park Road, Exeter, EX4 4QF

*Department of Aerospace Engineering, University of Bristol, University Walk,
Bristol, BS8 1TR

[†] Corresponding author Telephone: +44 (0)1392 263652 Fax: +44 (0)1392 264067

Abstract

Two-dimensional regular theoretical units that give a negative Poisson's ratio (NPR) are well documented and well understood. Predicted mechanical properties resulting from these models are reasonably accurate in two dimensions but fall down when used for heterogeneous real-world materials. Manufacturing processes are seldom perfect and some measure of heterogeneity is therefore required to account for the deviations from the regular unit cells in this real-life situation. Analysis of heterogeneous materials in three dimensions is a formidable problem; we must first understand heterogeneity in two dimensions. This paper approaches the problem of finding a link between heterogeneous networks and its material properties from a new angle. Existing optimisation tools are used to create random two-dimensional topologies that display NPR, and the disorder in the structure and its relationship with NPR is investigated.

Keywords

Heterogeneity, negative Poisson's ratio, optimisation

Introduction

A material with a negative Poisson's ratio (NPR), also termed an auxetic (Evans et al 1991), has the counter-intuitive property that it expands laterally when under tension and contracts when under compression. Materials with this property exist naturally (Lees et al 1991; Veronda and Westman 1970; Williams and Lewis 1982; Gunton and Saunders 1972; Baughman et al 1998) and have also been manufactured (Lakes 1987a; Lakes 1987b; Evans and Alderson 2000; Alderson and Evans 2001) from a variety of materials. The majority of synthetic auxetics can be classified as porous or 'cellular' in that they have large volume fractions of voids, notably polymer and metal foams (Bezazi and Scarpa 2007; Friis et al 1988) microporous polymers (Caddock and Evans 1989a; Caddock and Evans 1989b; Alderson and Evans 1992) and honeycombs (Masters and Evans 1996; Scarpa et al 2007; Gaspar et al 2005a). Auxetic materials have many potential applications but their manufacture is often problematic since the basis of most theoretical models of structure–property relationships require homogeneity and symmetry in the microstructure. This is possible with materials such as 2D honeycombs, although there are issues with manufacturing defects or in-service damage, but this is usually impossible with 3D cellular solids for instance polymeric foams, in which greater or lesser degrees of inhomogeneity and asymmetry exists in their microstructure. It is the purpose of this paper to explore the effects of heterogeneity on this structure-property relationship.

Much of the explicit modelling of cellular solids has considered tessellating, and therefore homogeneous, arrays of unit cells and uses simple beam mechanics to derive relationships between internal material properties and structure, and bulk properties (Gibson et al 1982; Evans and Grima 2000; Alderson and Evans 2001; Evans et al 1991; Gaspar et al 2005a; Sanders and Gibson 2003a; Sanders and Gibson 2003b; Lakes et al 1993). The results from these may correlate fairly well with experimental data but since their geometries often bear little resemblance to the reality of the internal microstructure of the materials there remains a gap in understanding between theorised ideals and the heterogeneous structures seen in auxetic materials (Gaspar et al 2005b). This disparity leads to difficulties in predicting properties when considering the manufacture of such materials since it is currently very difficult to accurately account for heterogeneity in microstructure and resulting Poisson's ratios (Gaspar et al 2005b; Koenders and Gaspar 2008). The issue of control over the nature and extent of heterogeneity is relatively unexplored and indeed may prove difficult to achieve in practice. However, previous work (Gaspar et al 2003) has shown that improved properties, and in particular negative Poisson's ratios, can be obtained from heterogeneous structures, but that the manufacture of such structures must be controlled closely.

Some work has been done to model heterogeneity, both for cellular solids (Guo and Gibson 1999; Silva et al 1995; Silva and Gibson 1997) and for fibrous composites (Yang et al 1999). This has predominantly taken the form of finite element models of specific anisotropic cell arrangements (Warren and Kraynik 1988; Warren and Kraynik 1991), rather than more generalised explicit forms. Other work (Gaspar et al

2003) has started to quantify numerically the differences in material properties (including calculations of material properties, failure modes and isotropy) between a homogeneous and a heterogeneous material.

The work described in this paper concerns the question of whether a 2D honeycomb with a microstructure optimised for negative Poisson's ratio in combination with a generally useful set of other elastic properties will be heterogeneous, and if so what are the underlying mechanisms engendering this negative Poisson's ratio. These questions are tackled via numerical optimisation of 2D grids and statistical analysis of results in the context of the homogenisation approach of Gaspar and co-workers (Gaspar et al 2003; Koenders and Gaspar 2008).

Methods

Two-dimensional grids with optimised honeycomb structures have been created using two different techniques. These have been optimised for maximal values of negative Poisson's ratio. The structures created were not assigned a specific material type since the internal geometry alone produces the NPR effect, as it does in most cases, meaning that the geometries could be applied to produce NPR in a wide range of materials. In practical applications, these could range from plastics and metals to carbon nanotubes, provided that the material itself remains in the linear elastic region so that the desired deformation mechanisms can function. Preliminary work on the two models presented here used values of Young's modulus ranging from 10 MPa to 70 GPa.

Two types of optimisation techniques were used, a genetic algorithm (GA) (Mitchell 1996; Davis 1991) and a differential evolutionary (DE) algorithm (Storn 1996; Mayer et al 2005). Both methods produce heterogeneous optimal solutions with negative Poisson's ratios but have different advantages; DEs efficiently explore a section of the possible solution surface (Pathria and Morris 1991; Lew et al 2006), whereas GAs are more computationally intensive but do not have pre-determined distributions for variables. The basis of the structures optimised is the Gibson-Ashby hexagon (Gibson and Ashby 1997) defined by h , t , ℓ and θ .

The genetic algorithm (GA) method was adapted from (Javadi et al 2005). A population of 10 identical arrays (10 by 10 cells, large enough to minimise edge effects but small enough to be computationally feasible) with $h=4\text{mm}$, $\ell=2.92\text{mm}$, $\theta=1.193\text{rads}$ (68.4°) and $t=0.2\text{mm}$ was created, known as generation 0, see Figure 1. The GA algorithm then applied random changes to the location of any or all of the nodes, and consequently the length of the ribs in each of the cells, creating 10 new different 'offspring' arrays. All offspring geometries were simulated under uniaxial loading in an FE package and the Young's moduli, Poisson's ratios and shear modulus of each data set were calculated. This was done in four stages, two uniaxial tensile tests and two shear tests. The FE package used was ABAQUS 6.5-5 (Dassault Systems) with beam elements of circular cross-section (diameter 0.2 units). Small displacements were applied to relevant sets of edge elements for the calculation of the grid's properties. These offspring are then evaluated for 'fitness' against a set of user-defined criteria, in this case for the maximum negative value of Poisson's ratio, where both ν_{21} and ν_{12} are being used for this assessment. The fittest members of each generation were then used as 'parents' for subsequent generations. The algorithm

iterates this process through a number of generations, each time improving against the criteria required. In addition to small random changes, the algorithm also allows periodic larger changes termed ‘mutations’, so the solution converges to the global optimum rather than becoming trapped in local minima.

The differential evolutionary algorithm (DE) method starts with one regular grid (see figure 2) defined by the user in terms of rib length ℓ and angle θ (again using the standard Gibson and Ashby notation as defined above). The user then defines a variance, the magnitude of the Gaussian distribution that governs the displacements of the nodes. The program then outputs a number (in this case 70) of random grids, representing the solution surface of the problem. The DE also uses the commercially available FEA package ANSYS (ANSYS Inc.) to find the Young’s moduli, Poisson’s ratios and shear modulus of each output. This was again done in four stages, two uniaxial tensile tests and two shear tests. The user must then evaluate manually to find the best solution from this set of possible solutions. There are 7 different variables available to the user every time the algorithm is run (starting rib length ℓ_0 , cell wall aspect ratio α , the angle defining the unit cell θ , the relative density β , the number of cells in the x -direction n , the variance, and the number of grids to output). For simplicity, the values of the cell wall aspect ratio α , the relative density β , and the starting rib length ℓ_0 , are all kept permanently to their default parameters of $\alpha=1.0$, $\beta=0.05$, $\ell_0=0.007$. The variances used for modifying the locations of the nodes were 5%, 10% and 15%. Figure 2 shows the three different starting geometries. The output parameters are E_1 , E_2 , ν_{21} , ν_{12} and G . The algorithm was asked to return 70 possible solutions each time.

The conventional statistical analysis of finding bulk material properties from local values concentrates on simply averaging local properties over the whole volume (mean-field approximation). This homogenisation process loses potentially important information regarding particular parts of the material. It is the purpose of this study to work towards ascertaining what the parameters that affect NPR are, and therefore, such generalisation is not very useful.

The geometry of the grid can be defined by the locations of the nodes, or by the length of the ribs r connecting the nodes and the angles θ between them. Preliminary statistical calculations were performed on the lengths and angles. More sophisticated techniques were then used to further interrogate the structure of these simulated grids. The following techniques are based on analyses of randomly packed granular materials that have been adapted to bending beam networks (Koenders and Gaspar 2008).

If we consider stiffness tensor Z for these 2D arrays then locally, for each node μ the elastic properties are related by

$$\sigma^\mu = Z^\mu \varepsilon^\mu \quad (1)$$

and globally the properties arise as an average of the local properties, i.e. $\bar{\sigma} = \bar{Z}\bar{\varepsilon}$ (where $\bar{\sigma}$ and $\bar{\varepsilon}$ are the local stress strain respectively, the bar denoting 'local') so under equilibrium conditions at any point μ $\sigma^\mu = \bar{\sigma}$. However, due to the heterogeneity in the structures, the global properties are not the same as an average of the local properties (Gaspar et al 2003), therefore, an additional term based on the geometrical differences must be included. The analysis follows that of Koenders and Gaspar (2008) in which each node is considered subject to force and force moments

from the displacements of its neighbours. Neighbours v are located a vector $\underline{c}^{\mu v}$ from node μ . The mechanics of the geometry then entrain summations over neighbouring nodes. These so-called structural sums represent the fabric of the material.

These structural sums can then be used to find the constant strain mean-field approximation, ie the stiffness tensor Z , from the equilibrium equations solved for the specific geometry. The Poisson's ratio can then be calculated (table 1).

$$Z_{pqij}^{\mu} = P_{ijst}^{\mu} A_{pstq}^{\mu} \quad (2)$$

Where the summation convention holds for repeated indices and

$$A_{pijk}^{\mu} \equiv \sum_{v=1}^{N^{\mu}} [(Esc)^{\mu v} n_i^{\mu v} n_j^{\mu v} n_k^{\mu v} n_p^{\mu v}] + 12 \sum_{v=1}^{N^{\mu}} \left[\left(\frac{EI}{c} \right)^{\mu v} \bar{n}_i^{\mu v} n_j^{\mu v} n_k^{\mu v} \bar{n}_p^{\mu v} \right] \quad (3)$$

$$P_{ijkl}^{\mu} = \delta_{ij} \delta_{kl} + \varepsilon_{ij3} \Phi_{kl} \quad (4)$$

where E is the Young's modulus, s the sectional area, c the rib length, I the second moment of area, and

$$\Phi_{ij}^{\mu} = \frac{\sum_{v=1}^{N^{\mu}} \left[\left(\frac{EI}{c} \right)^{\mu v} n_j^{\mu v} \bar{n}_i^{\mu} \right]}{\sum_{v=1}^{N^{\mu}} \left(\frac{EI}{c} \right)^{\mu v}} \quad (5)$$

δ_{xy} is the Kroenecker delta

ε_{ijk} is the permutation tensor

and

n is the unit vector connecting nodes μ and ν

To this is then added a corrective term (highlighted) that takes local heterogeneity into account:

$$\sigma = (\bar{Z} + \underline{\bar{Z}'X})\bar{\varepsilon} \quad (6)$$

The complete corrective term, taken from the full explicit calculation (Koenders 2005), is based upon allowing local deformations to the nodes and then requiring equilibrium in force and moments.

$$Z'_{pqbc}{}^{\mu} U'_{(bc)}{}^{\mu} = -\frac{1}{4\pi\zeta} \left(P'_{bcst}{}^{\mu} \langle A \rangle_{pqst} + \langle P \rangle_{bcst} A'_{pqst}{}^{\mu} \left(\frac{\zeta}{\kappa + 2\zeta} (A'_{bijc}{}^{\mu} + A'_{cijb}{}^{\mu}) - \frac{\kappa + \zeta}{\kappa + 2\zeta} A'_{aija}{}^{\mu} \delta_{bc} \right) \right) \langle P \rangle_{ijef} \langle U^1 \rangle_{(ef)} \quad (7)$$

where

U is the local continuum rotation, and subscripts bc and ef denote a symmetrised tensor.

ζ and κ are Lamé's constants

Results

The values of the Poisson's ratios from the arrays generated by one run of the GA optimiser can be seen in figure 3, and most other runs were similar. All the results were heterogeneous, strongly suggesting that heterogeneous grids have advantageous

properties over homogeneous counterparts. Large changes occur at the beginning, then as the solution progresses it becomes asymptotic towards an optimum. The data are for the fittest member in each generation. These data do not necessarily end with the most negative values as the process is iterative and may also produce a less fit generation than the preceding one.

Fig 4 shows the starting grid and a selection of subsequent optimised grids, along with the Poisson's ratio ν_{21} . The properties of the starting grid were obtained from FE analysis on a regular hexagonal unit cell. It is interesting to note that there is no obvious visible difference between generation 1 and generation 800 despite the large difference in Poisson's ratio between them. It is clear that subtle changes in geometry are having a very large effect on the properties.

Very large negative values (up to -6.83) of Poisson's ratio were obtained from the DE with a starting grid of $\theta = -5^\circ$. In addition, Poisson's ratios of approximately 1 were produced with $\theta = 30^\circ$. However, the most interesting results come from a starting grid of $\theta = 0^\circ$ as the resulting arrays include both positive and negative Poisson's ratio examples, see Figure 3, and, as with the GA, there is no obvious difference between these structures.

The off-axis properties can be calculated from the conventional equations (Nye 1957), and are given in Figure 5. For simplicity, only the two most negative results are shown, one from the GA and one from the DE. The off axis Poisson's ratios from the DE are all negative, which contrasts with those from the GA which are predominantly positive. There is also more variation in the Poisson's ratios obtained from the DE

(-5.68 to -0.01) when compared with the GA (-0.34 to 0.65). The frequency of radius and angle for maximum and minimum Poisson's ratio cases for the DE and GA are presented in Figures 6 and 7 respectively.

In addition to neighbour-neighbour considerations, correlations between non-contacting ribs were also investigated. Ribs with angles greater than 6° from the vertical or from the horizontal were correlated with all other ribs. The ribs which are almost perfectly horizontal or vertical are a priori well correlated. By removing them with a minimum angle stipulation we concentrate on the ribs whose geometry provides the most variation between models. Figure 8 shows a pair of non-contacting ribs, which are treated as vectors V_1 and V_2 , the distance between them, r , and the angle between them θ . The sign of the angle θ defined here depends on which rib in a pair is chosen as V_1 , and on the orientation of the vectors. The function $\cos(2\theta)$ removes these dependencies.

These values were then used in a set of correlation functions, β . The most interesting were found to be:

$$\text{Double angle} \quad \beta = \cos(2\theta) \quad (8)$$

$$\text{Mixed angle} \quad \beta = |V_1||V_2|\cos(2\theta) \quad (9)$$

These functions were then used to analyse the data from the DE. The correlation functions are plotted in Figure 9 as a function of separation r for the DE results with $\theta=0$.

Discussion

The most interesting outcome so far arises from the DE results and it is that larger negative values of global Poisson's ratio were obtained with lower variance values than with larger variance values (Figure 5). This somewhat surprising result underlines the observation that subtle structural changes may make very large differences in Poisson's ratio, but also that these subtle structural changes must be of a particular type (as yet unquantified). Since Poisson's ratios in cellular solids are almost wholly dependent on microstructure rather than the properties of the constitutive material, this finding has implications for foams, honeycombs and other cellular solids, fabricated from many different materials, and used in a wide range of applications.

The constant strain mean-field approximation for the GA structures, table 1, predicts no negative values of Poisson's ratio, yet we know from the FEA that the structures do in fact have NPR. This reinforces the idea that subtle structural changes can have a large effect on the value of Poisson's ratio. Quantifying such changes would allow material properties to be tailored to specific requirements, but the accuracy of the predictive mean-field approximation is not yet sufficient for this to occur. Despite attempts to correlate heterogeneity measures with elastic parameters such as Poisson's ratio, in such materials, there is as yet no known robust method for doing this [Gaspar and Koenders, 2001b; Kuhn 2003]. In contrast to the mean-field approximation, the full corrective term shows too large a value of NPR. If we look more closely at the standard deviation of the corrective term, we can see that it is approximately 50%. The corrective term in Koenders (Koenders 2005) presumes only first order

fluctuations in the displacement fields applied, and we can see that these assumptions are breaking down, i.e. the fluctuations in the grids are too big to directly compare with the theoretical calculations. This shows that either the optimisation tools must apply an unintended constraint on the extent of heterogeneity, or these calculations need to be extended to accommodate larger fluctuations. However, this analysis is still valid in the calculation of the shear modulus [Gaspar and Koenders, 2001a], where similarly there is no correlation between the mean-field approximation prediction and the statistical measures of rib-lengths and angles.

The DE data has also been analysed with the full mean-field approximation and corrective term calculations, with worse correlations found than with the GA. In addition, the same results have been found as with the GA regarding the frequency distributions of the rib lengths. That is, that there is no difference between the two (Figure 6). These results were contrary to those that have been found from previous similar work (Gaspar et al 2005b) which always found obvious differences between positive and negative Poisson's ratio structures. Although Gaspar *et al* analysed 3D NPR foams whereas the present structures are 2D, there seems to be no *a priori* reason why similar shifts in peak frequency values should not also be seen in the present structures if the same factors underlay the changes in Poisson's ratio.

Koenders and Gaspar (Koenders and Gaspar 2008) also propose a partial corrective term as an alternative to the full calculation

$$Z_{1122}^{corr} = -\frac{8\pi\langle P_{12}^2 \rangle}{3} \times \zeta \quad (9)$$

Looking at this equation, we can see that Z_{1122}^{corr} has a predominant dependency on the $\langle P_{12}^2 \rangle$ term. However, this partial correction is based on the assumption that all the ribs are long and slender. Looking at the rib lengths in these results (figure 7) we can see that this assumption is definitely not valid in this case. Indeed, with a diameter of 0.2, not an insignificant number of the connections between the nodes are shorter than this. Looking at table 2 we can see the effect of having a node with a shorter rib attached has on $\langle P_{12}^2 \rangle$. Therefore, this issue has to be addressed by constraining the GA so that there is a specified minimum aspect ratio.

In addition, looking at the off-axis properties, it can clearly be seen that the DE is optimising in one direction, hence the anisotropy in the Young's modulus when compared with the off-axis values from the GA, where very similar values are obtained at both 0° and 90° . This also leads to very negative values of Poisson's ratio (minimum off-axis value of -5.68). Interestingly, in addition, the off-axis Poisson's ratio is entirely negative. This again is in stark contrast to the GA where both positive and negative values occur. Theoretically, the GA should produce the more negative results as it should optimise for the most negative value of Poisson's ratio in one direction. Whilst this is true for the on-axis case, when taking all orientations into consideration this is no longer the case.

The interactions between non-contacting pairs of ribs gives more of an insight into why these measures of heterogeneity tend not correlate well with predictions of elastic

constants. In Figure 9 where $r \cdot 100 = 1$ the separation r is approximately equivalent to one rib length and thus equivalent to the above neighbour-neighbour interactions (simple rib-length and angle correlations and the mean-field approximation). At these short length scales it is clear that there is very little correlation between angles, and it is only when distances increase to about 3-12 rib lengths that we see a marked increase correlation (β) for both the PPR and NPR cases. This would indicate that the effective unit cell, i.e. the functional unit of deformation, may be significantly larger than the individual honeycomb cells. This may explain why NPR mechanisms have been difficult to uncover in these structures. This larger effective unit cell has also been found in granular mechanics, and is sometimes referred to as structure formation [Koenders, 1997] or as a circulation cell [Williams and Rege, 1997].

Conclusion

Two different optimisation tools have been introduced and their results analysed. Heterogeneous grids are created by both methods, showing that a negative Poisson's ratio honeycomb can be created simply by adding disorder to a positive Poisson's ratio one. Both optimisation tools have different advantages and offer different insights into heterogeneity, although no direct predictive relationship between heterogeneity and such elastic properties had been found as yet despite some work towards this [Gaspar and Koenders, 2001b; Kuhn 2003], although the mean-field approximation is still of use in predicting the shear moduli. Negative values of Poisson's ratios were found in both cases and the statistical tools are in place for work to continue on quantifying the relationship between heterogeneity and material properties. Further work will investigate higher order interactions, i.e. longer length

scale interactions between non-contacting neighbours, since the effective unit cell appears to be much larger than first thought. A robust direct correlate of structural heterogeneity and mechanical properties in such structures may well result.

References

ABAQUS 6.5-5, Dassault Systems, Providence, RI, USA, 2007

Alderson A and KE Evans “Rotation and Dilation Deformation Mechanisms for Auxetic Behaviour in the α -cristobalite Tetrahedral Framework Structure” *Physics and Chemistry of Minerals* (2001) 28, pp 711-718

Alderson KL and KE Evans “The Fabrication of Microporous Polyethylene Having a Negative Poisson’s Ratio” *Polymer* 33 (20) 1992, pp 4435-4438

ANSYS 11.0, ANSYS Inc, Canonsburg, PA, USA, 2007

Baughman RH, JM Shacklette, AA Zakhidov and S Stafstrom “Negative Poisson’s Ratios as a Common Feature of Cubic Metals” *Nature* 392, 1998, pp 362-365

Bezazi A and F Scarpa “Mechanical Behaviour of Conventional and Negative Poisson’s Ratio Thermoplastic Polyurethane Foam Under Compressive Cyclic Loading” *International Journal of Fatigue* Vol. 29, No. 5 May 2007, pp 922-930

Caddock BD and KE Evans “Microporous Materials with Negative Poisson’s Ratios 1: Microstructure and Mechanical Properties” *Journal of Physics D: Applied Physics* 22 (12) December 1989, pp 1877-1882

Davis L “Handbook of Genetic Algorithms” Van Nostrand Reinhold, USA 1991

Evans KE, MA Nkansah and IJ Hutchinson “Molecular Network Design” *Nature* 353 September 1991, pp 124

Evans KE and A Alderson “Auxetic Materials: Functional Materials and Structures from Lateral Thinking” *Advanced materials* 2000, 12 Vol. 9, pp 617-627

Evans KE and JN Grima “Auxetic Behaviour from Rotating Squares” *Journal of Material Science Letters* 19, 2000, pp 1563-1565

Friis EA, RS Lakes and JB Park “Negative Poisson’s Ratio Polymeric and Metallic Foams” *Journal of Materials Science* 23 (12) December 1988, pp 4406-4414

Gaspar N and Koenders MA “Micromechanic Formulation of Macroscopic Structures in a Granular Medium” *Journal of Engineering Mechanics*, Vol. 127, Issue 10, 2001a, pp 987-993

Gaspar N and Koenders MA “Estimates of the Shear Modulus of a Granular Assembly using Heterogeneous Media Techniques” *Powders and Grains*, pp165-168, 2001b

Gapsar N, CW Smith, KE Evans “The Effect of Heterogeneity on the Elastic Properties of Auxetic Materials” *Journal of Applied Physics* 94 (9) November 2003, pp 6143-6149

Gaspar N, XJ Ren, CW Smith, JN Grima, KE Evans “Novel Honeycombs with Auxetic Behaviour” *Acta Materialia* Vol. 53, No. 8, May 2005a, pp 2439-2445

Gaspar N, C W Smith, E A Behne, G T Seidler, K E Evans “Quantitative Analysis of the Microscale of Auxetic Foams” *Physica Status Solidi B* 242 No.3 2005b, pp 550-560

Gibson LJ, MF Ashby and GS Schajer “The Mechanics of Two-Dimensional Cellular Materials” *Proceedings of the Royal Society of London A* 382, 1982, pp 22-45

Gibson LJ and MF Ashby “Cellular Solids: Structure and Properties” Cambridge University Press, Cambridge 1997 pp105

Gunton DJ and GA Saunders “Young’s Modulus and Poisson’s Ratio of Arsenic, Antimony and Bismuth” *Journal of Materials Science* 7 (9) 1972, pp 1061

Guo XE and LJ Gibson “Behaviour of Intact and Damaged Honeycombs: A Finite Element Study” *International Journal of Mechanical Sciences* 41 1999, 85-105

Javadi AA, R Farmani and TP Tan “A Hybrid Intelligent Genetic Algorithm” *Advanced Engineering Informatics* 19, 2005, pp 255-262

Koenders MA “Constitutive Properties of Contacting Materials with a Finite-Sized Microstructure” *Molecular Simulation* Vol. 13 No. 13 November 2005, pp 837-882

Koenders MA and Gaspar N “The Auxetic Properties of a Network of Bending Beams.” *Physica Status Solidi b*, 245, No.3, 2008, pp 539-544

Kuhn MR, “Heterogeneity and Patterning in the Quasi-Static Behaviour of Granular Materials,” *Granular Matter*, Vol. 4, No. 4, pp. 155-166, 2003.

Lakes R “Foam Structures with a negative Poisson’s ratio” *Science* 235, 1987a, pp 1038-1040

Lakes R, Patent Application PCT/US87/01148 Polyhedron Cell Structure and Making of the Same, 1987b

Lakes R, P Rosakis, A Ruina “Microbuckling Instability in Elastomeric Cellular Solids” *Journal of Material Science* Vol. 28, No. 17, September 1993, pp 4667-4672

- Lees C, JFV Vincent and JE Hillerton "Poisson's Ratio in Skin" *Bio Medical Materials and Engineering* (19) 1991, pp 19-23
- Lew TL, AB Spencer, F Scarpa, K Worden, A Rutherford, F Hemez "Identification of Response Surface Models Using Genetic Programming" *Mechanical Systems and Signal Processing* 20, 2006, pp 1819-1831
- Masters IG and Evans KE "Models for the elastic deformation of honeycombs" *Composite Structures*, Vol. 35, Issue 4, August 1996, pp 403-422
- Mayer DG, BP Kinghorn, AA Archer "Differential Evolution-An Easy and Efficient Evolutionary Algorithm for Model Optimisation" *Agricultural Systems* Vol. 83 Issue 3 March 2005, pp 315-328
- Mitchell M "An Introduction to Genetic Algorithms" MIT Press, USA 1996
- Nye JF "Physical Properties of Crystals" Oxford University Press, Oxford, 1957, Chapter 8.
- Pathria D and JL Morris "A Variable Spectral Collocation Algorithm for the Solution of Non-Linear Evolutionary Equations" *Applied Numerical Mathematics*, Vol. 8 Issue 3 October 1991, pp 243-256
- Sanders WS and LJ Gibson "Mechanics of BCC and FCC Hollow Sphere Foams" *Materials Science and Engineering A383* (2003a), pp 150-161
- Sanders WS and LJ Gibson "Mechanics of Hollow Sphere Foams" *Materials Science and Engineering A347* (2003b), pp 70-85
- Scarpa F, S Blain, T Lew, D Perrott, M Ruzzene, JR Yates "Elastic Buckling of Hexagonal Chiral Cell Honeycombs" *Composites Part A (Applied Science and Manufacturing)* Vol. 38, Issue 2, 2007, pp 280-289
- Silva MJ, WC Hayes and LJ Gibson "The Effects of Non-Periodic Microstructure on the Elastic Properties of Two-Dimensional Cellular Solids" *International Journal of Mechanical Sciences* Vol. 37 No.11 1995, pp 1161-1177
- Silva MJ and LJ Gibson "The Effects of Non-Periodic Microstructure and Defects on the Compressive Strength of Three-Dimensional Cellular Solids" *International Journal of Mechanical Sciences* Vol. 39, No. 5 1997, pp 549-563
- Storn R "On the use of differential evolution for function optimisation" NAPHIS, 1996
- Veronda DR and RA Westmann "Mechanical Characterization of Skin-Finite Deformations" *Journal of Biomechanics* 3 (1) 1970, pp 111
- Warren WE and AM Kraynik "The Linear Elastic Properties of Open-Cell Foams" *Journal of Applied Mechanics* 55 1988, pp 341-346

Warren WE and AM Kraynik “The Nonlinear Elastic Properties of Open-Cell foams”
Journal of Applied Mechanics 58 1991, pp 376-381

Yang S, AM Gokhale and Z Shan “Utility of Microstructure Modelling for
Simulation of Micro-Mechanical Response of Composites Containing Non Uniformly
Distributed Fibres” Acta Materialia 48 1999, pp 2307-2322

ACCEPTED MANUSCRIPT

TABLES

Table 1 Poisson's ratios obtained from the GA runs by averaging the material properties, correcting this average to account for the heterogeneity, and from the FE analysis.

	Poisson's ratio ν_{21}		
Generation	Uncorrected (mean-field)	Corrected	FE simulation
1	0.2585	-0.3012	0.0474
10	0.2074	-0.2431	-0.0538
800	0.2378	-0.2131	-0.200

Table 2: $\langle P_{12}^2 \rangle$ values for short and long ribs

Generation	$r < 1.0$	$r > 1.0$
1	0.51659	0.31283
10	0.50067	0.32577
800	0.38843	0.32570

Figure 1 Starting grid for the GA ($\nu_{12} = 0.714$, $\nu_{21} = 0.855$)

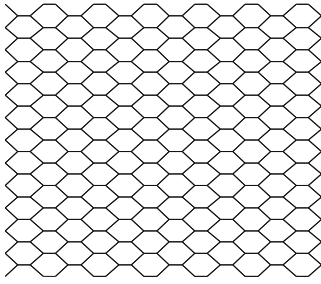
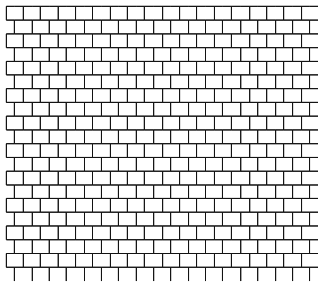
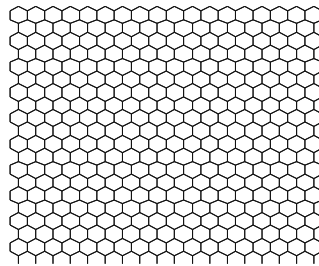


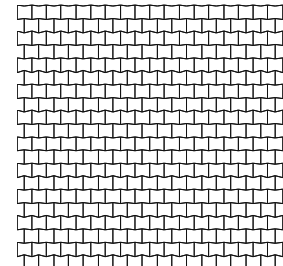
Figure 2 Starting grids for DE showing the different starting angles



$\theta = 0^\circ$



$\theta = 30^\circ$



$\theta = -5^\circ$

Figure 3: Poisson's ratio by generation (GA) and average values with min/max bars (DE)

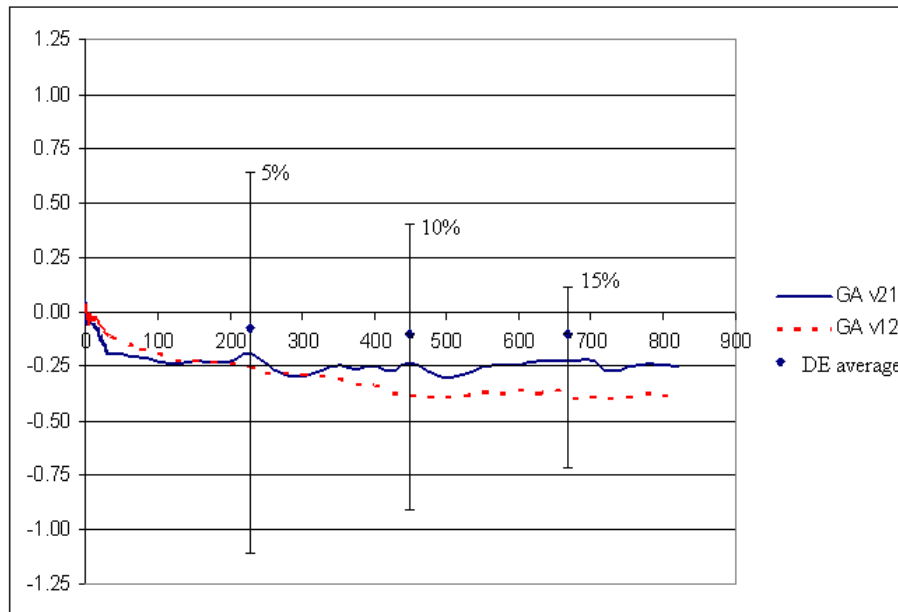
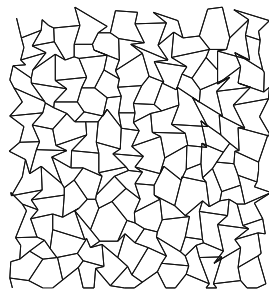
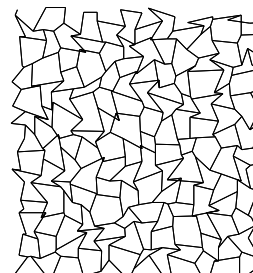


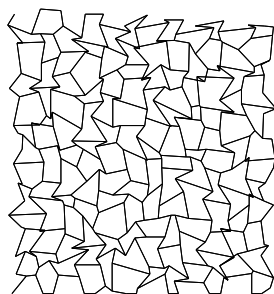
Figure 4 Starting grid and subsequent optimised grids by generation



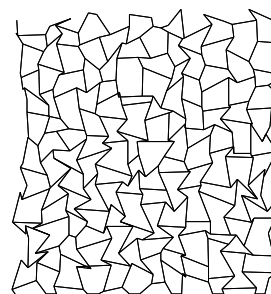
Generation 1 $v_{21} = 0.0474$



Generation 2 $v_{21} = 0.0106$

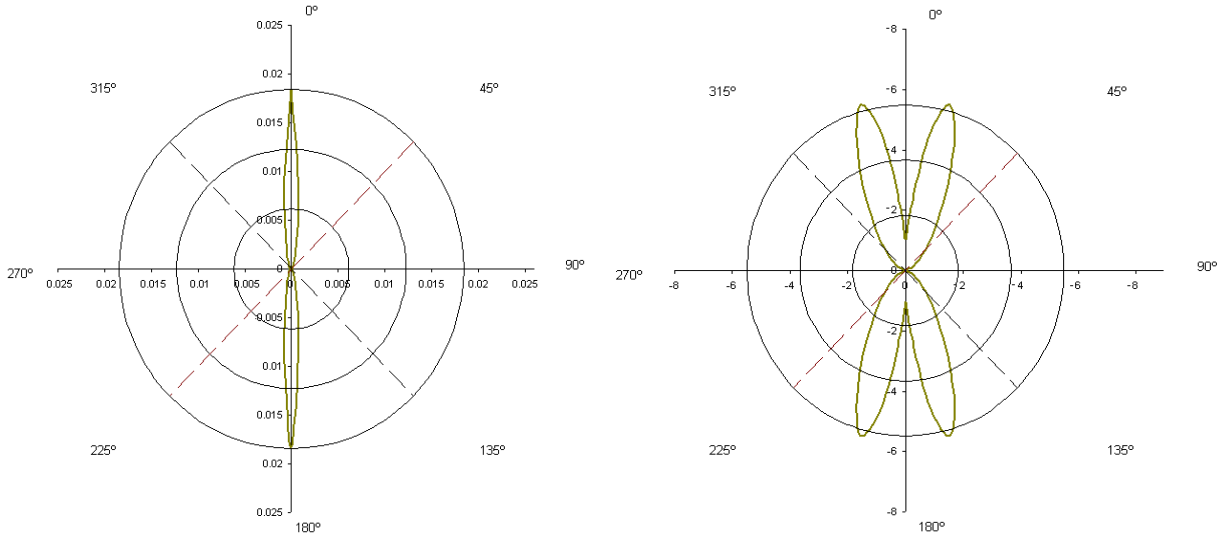


Generation 10 $v_{21} = -0.0538$



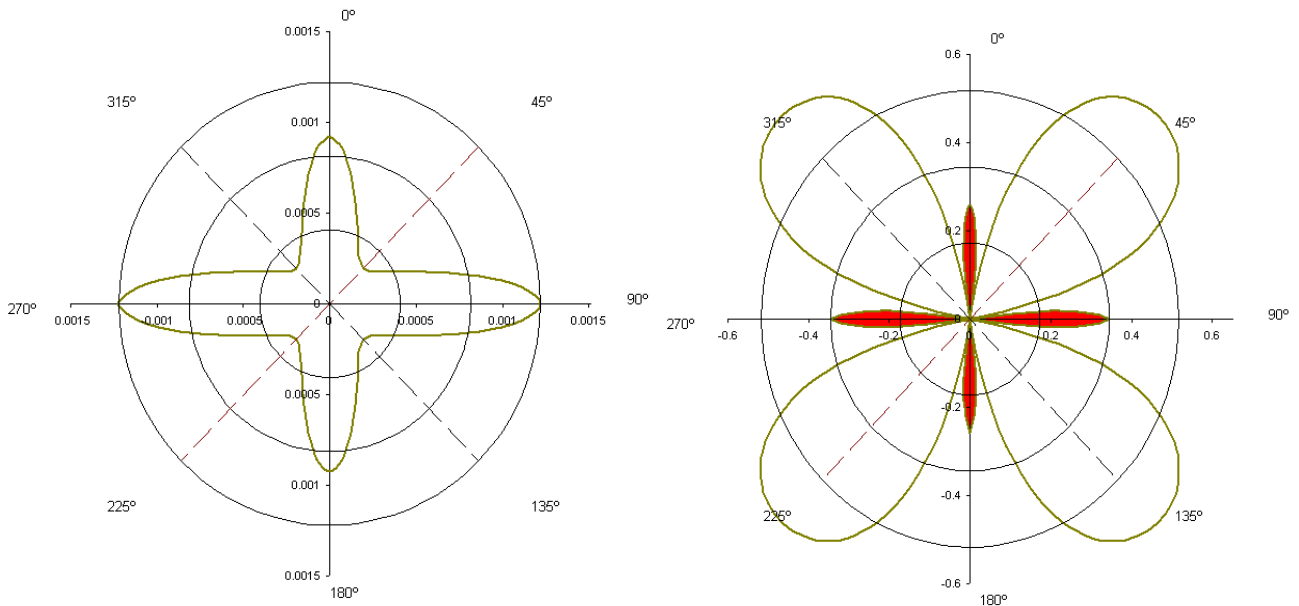
Generation 800 $v_{21} = -0.253$

Figure 5: Off-Axis properties for GA and DE data

DE results for $\theta=0$, variance=5%, $v_{21}(\text{on-axis})=-1.0395$ 

Young's Modulus (normalised to constituent material)

Poisson's Ratio

GA results for generation 800 $v_{21}(\text{on-axis})=-0.200$ 

Young's Modulus (normalised)

Poisson's Ratio (negative values shaded)

Figure 6: Frequency of radius and angle for maximum and minimum Poisson's ratio cases for the DE

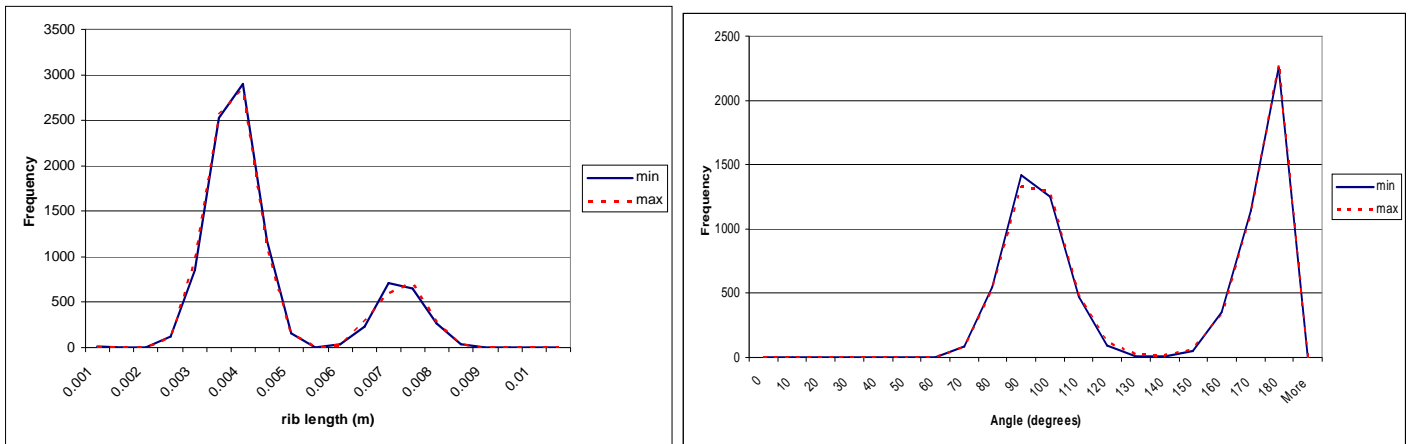


Figure 7 Rib length against frequency for the GA

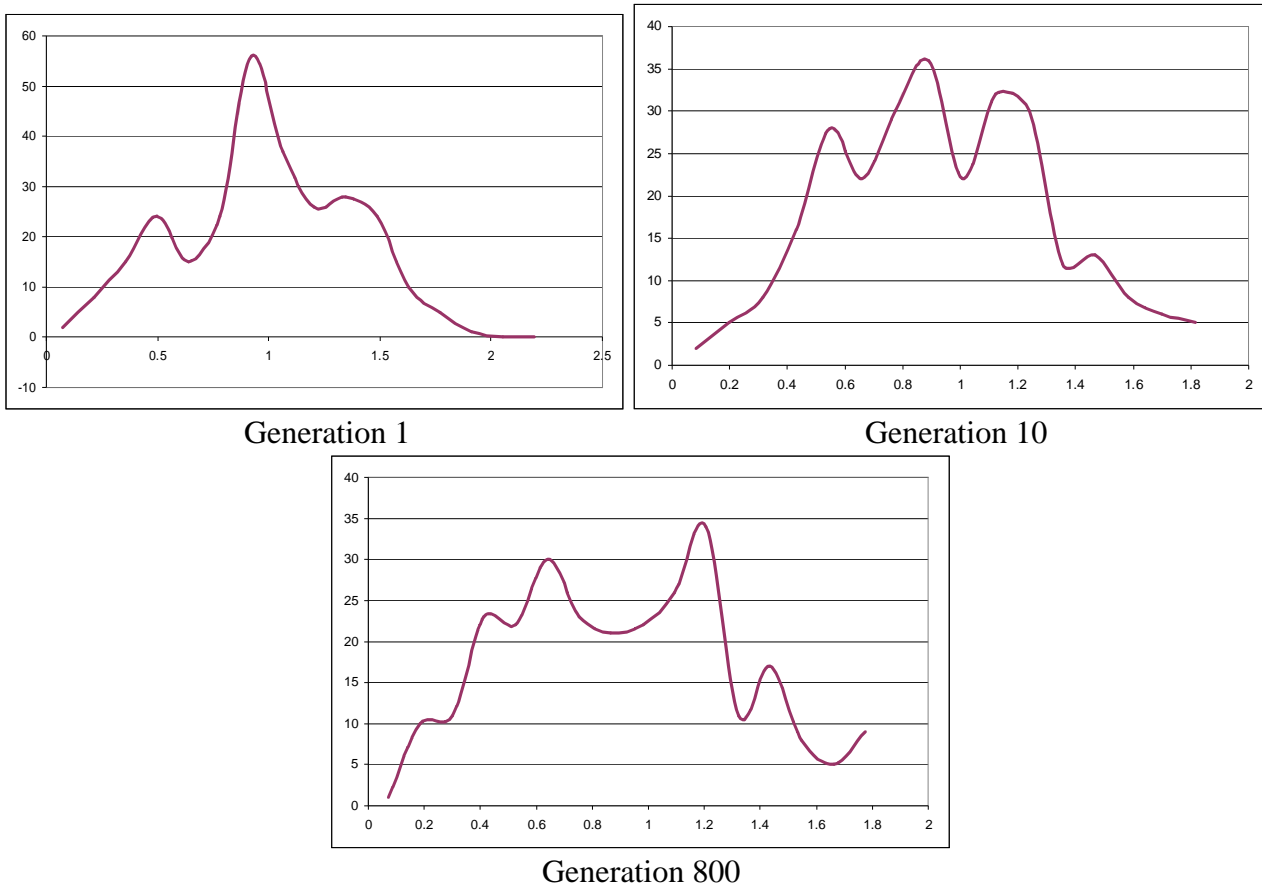


Figure 8: Showing notation for non-contacting rib pairs

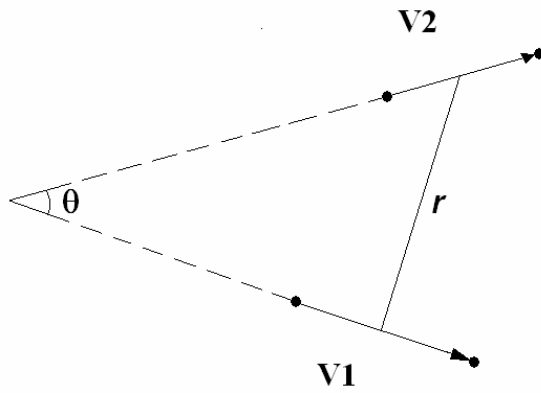


Figure 9: Correlation functions as defined in equations 7 and 8

